TSINGHUA SCIENCE AND TECHNOLOGY
ISSN 1007-0214 01/11 pp 1– 8
DOI: 10.26599/TST.2018.9010065
Volume 24, Number 1, February 2019

Interface Electric Field Confinement Effect of High-Sensitivity Lateral Ge/Si Avalanche Photodiodes

Wenzhou Wu, Zhi Liu, Jun Zheng, Yuhua Zuo, and Buwen Cheng*

Abstract: A novel lateral Ge/Si avalanche photodiode without a charge region is investigated herein using device physical simulation. High field is provided by the band-gap barrier and build-in field at the Ge/Si interface in the vertical direction. Modulating the Si mesa thickness ($0-0.4\,\mu\mathrm{m}$) and impurity concentration of the intrinsic Si substrate ($1\times10^{16}-4\times10^{16}\,\mathrm{cm}^{-3}$) strengthens the electric field confinement in the substrate region and provides a high avalanche multiplication in the Si region. When the Si mesa thickness is $0.3\,\mu\mathrm{m}$, and the impurity concentration of the Si substrate is $2\times10^{16}\,\mathrm{cm}^{-3}$, the Lateral Avalanche PhotoDiode (LAPD) exhibits a peak gain of 246 under $1.55\,\mu\mathrm{m}$ incident light power of $-22.2\,\mathrm{dBm}$, which increases with decreasing light intensity.

Key words: avalanche photodiodes; lateral structure; electric field confinement; high gain

1 Introduction

The research interest on high-performance Avalanche PhotoDiodes (APDs), which exhibit an internal carrier multiplication mechanism caused by internal avalanche gain[1–5], has been increasing with the development of optical fiber communication. APDs must have a very low noise and a high response to increase sensitivity in low-light-level detection. The electron impact ionization rate of Si is 100 times larger than the hole impact ionization rate; hence, using Si as the multiplication material can result in a higher gain and a very low excess noise during detection[6,7]. Ge APDs based on a high-quality Ge epitaxy on Si can easily detect the weak signals in the near-infrared wave band, which includes the $1.55\,\mu\mathrm{m}$ wavelength used for fiber communication[4,5,8,9]. Ge APDs are easy to realize on a Si substrate because of the similarities in the crystal structure of Ge and Si. Furthermore, Ge APDs are compatible with conventional complementary metal-oxide-semiconductor processing, which makes optoelectronic monolithic integration easier to realize. As shown in the work of Duan et al.[10], Ge/Si APD structures can achieve gain above 40 after an appropriate structure optimization using a $0.5\,\mu\mathrm{m}$-thick multiplication layer.

According to Abou El-Ela and Hamada[11], the avalanche gain of semiconductor material increases with the increase in the electric field in the multiplication region. Moreover, the avalanche multiplication process is significantly enhanced when the electric field is larger than 130 kV/cm in Ge and 330 kV/cm in Si. Thus, the electric field confinement in Ge/Si APD is important in obtaining high gain[11,12]. A high electric field confinement in Separate Absorption, Charge, and Multiplication (SACM) APDs is modulated by the charge layer. When an APD reaches its breakdown voltage, the electric field in the avalanche region starts to decrease because of the space charge effect, whereas that in the absorption region keeps rising simultaneously, resulting in a sharp decrease in the gain[13]. The decreasing electric field

• Wenzhou Wu, Zhi Liu, Jun Zheng, Yuhua Zuo, and Buwen Cheng are with the State Key Laboratory on Integrated Optoelectronics, Institute of Semiconductor, Chinese Academy of Sciences, Beijing 100083 and the College of Materials Science and Opto-Electronic Technology, University of Chinese Academy of Sciences, Beijing 100049, China. E-mail: wuwenzhou@semi.ac.cn; zhiliu@semi.ac.cn; zhengjun@semi.ac.cn; yhzuo@semi.ac.cn; cbw@semi.ac.cn.
* To whom correspondence should be addressed.
Manuscript received: 2017-03-02; revised: 2017-03-22; accepted: 2017-03-23

in the avalanche region in the SACM APD restricts the possibility of a higher gain[8,9]. Thus, a better mechanism of field confinement in APDs is the key for obtaining a higher gain.

This study theoretically analyzes a new structure for a Lateral Avalanche PhotoDiode (LAPD) using a novel electric confinement mechanism based on the device physical simulation software of lumerical FDTD and DEVICE solutions. As shown in Fig. 1, the LAPD is different from a conventional LAPD in structure, and no electrode is present in the Ge region[4,14]. Our structure also has a unique Si mesa in the Ge absorption region to modulate the field distribution in the device. The simulation shows a substantial improvement in the avalanche gain using our LAPD compared with the conventional SACM APDs of the same multiplication length.

2 Parameter Settings

Figure 1 shows the schematic of the device analyzed in this study. The substrate was a 0.3 μm-thick silicon-on-insulator, and the intrinsic area of the Si substrate was maintained at $7 \times 10\,\mu m^2$. The $2 \times 10\,\mu m^2$ highly p^+- and n^+-doped Si regions were set on the left and right sides of the substrate, respectively. The 0.5 μm-thick Ge absorption region was set at the center top of the Si substrate with an area of $6 \times 10\,\mu m^2$, leaving two 0.5 μm-long intrinsic Si gaps on both sides of the Ge mesa. We refer to the gap between the Ge mesa and the p^+-doped region as gap A, and the one between the Ge mesa and the n^+-doped region as gap B. An epitaxial Ge usually appears to be a weak p-type because of the defects in the epitaxy layer[15]. The impurity concentrations of Ge and the highly doped region were set as 5×10^{15} cm^{-3} and 1×10^{20} cm^{-3}, respectively. From the simulation, a built-in field was formed by setting the impurity of the Si substrate as an n-type at the Ge/Si interface, which enhanced the electric field redistribution in Ge.

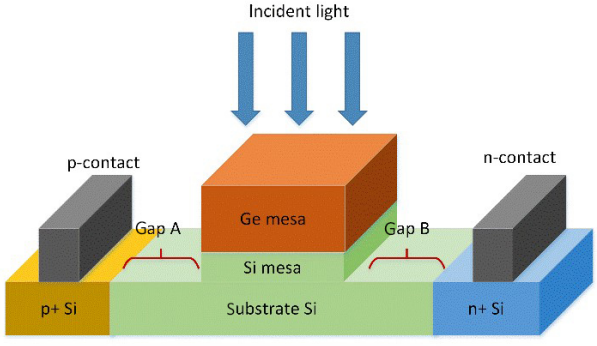

Fig. 1 Three-dimensional schematic of the lateral Ge/Si APD without a charge region.

We simulated the structure with the substrate for various impurity concentrations. The concentration was varied from 4×10^{12} to 4×10^{16} cm^{-3}, and the corresponding square resistance varied from 1000 Ω to 0.2 Ω[16]. In practical applications, the impurity concentration of the device can be controlled through the selection of a wafer with a suitable square resistance. During the simulation, adding a Si mesa under the Ge mesa produced a good electric field modulation effect. The thickness of the Si mesa under the Ge mesa was increased from 0 to 0.3 μm to analyze the field modulation in the structure when the area of the Si mesa was the same as that of the Ge mesa.

The Ge/Si interface was full of defects, which can result in a carrier recombination through the Ge/Si interface[17]. Moreover, a carrier recombination occurred at the semiconductor/insulator interface around the device because of the existence of surface-dangling bonds on the semiconductor surface[18]. We used the surface recombination velocity mentioned in Yablonovitch et al.[19] to ensure that the simulation closely mimics the real device. The surface recombination velocities on the Ge/Si interface and the semiconductor/insulator interface in the lateral region of the LAPD were set as 1×10^3 cm/s and 1×10^7 cm/s in the program, respectively.

3 Device Characteristics and Discussion

Figure 2 presents the I-V curve of the LAPD with an impurity concentration of $N = 2 \times 10^{16}$ cm^{-3} and a Si mesa thickness of $T = 0\,\mu m$. The light current in the region biased from 0 V to −22 V was only 20 nA because the device had a long intrinsic region of 7 μm. As shown in Fig. 3, the electric field in gap A at −23 V was high enough to trigger an avalanche ionization. When the bias was lower than −22 V, the intrinsic region did not punch through, and the photo-generated carriers were blocked, resulting in a relatively low photocurrent. When the bias was above the punch-through voltage of −22 V, the holes generated by the avalanche ionization drifted into the high-field region in gap A. The gain of the device sharply rose and reached a peak at −23 V. When the bias kept rising, the electric field in the mid-intrinsic region increased, whereas

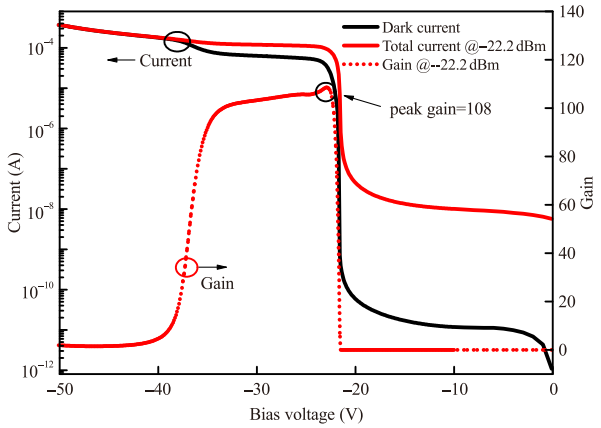

Fig. 2 ***I-V*** **and avalanche gain curves of the LAPD. Si mesa thickness** $T = 0$ **μm and substrate Si impurity concentration** $N = 2 \times 10^{16}$ **cm^{-3} under –22.2 dBm light.**

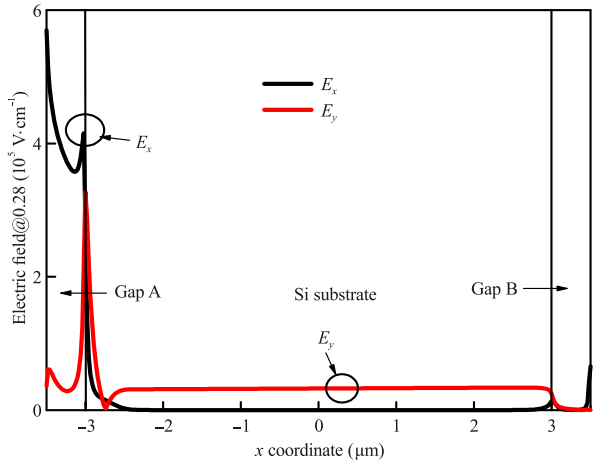

Fig. 3 E_x **and** E_y **distribution in the substrate intrinsic region at** $y = 0.28$ **μm and** -23 **V.**

that in gap A slowly decreased because of the space charge effect. The device did not have a steep gain peak because of the difference in the mechanism of the field confinement from the SACM APD. The dark current at -23 V was 5.93 μA, and the gain was 108 under an incident light power of -22.2 dBm at 1.55 μm. For comparison, we also analyzed a classic vertical SACM APD structure under the same simulation condition. The radius of the vertical SACM APD was 4.5 μm, and the lengths of the absorption and multiplication regions were 0.5 μm. The peak gain of the vertical SACM APD was 69 under -22.2 dBm, and the dark current at the peak gain voltage was 12.7 μA.

From the simulations, the novel LAPD structure without a charge region for field isolation exhibited a good gain and relatively low dark current. In other words, the novel LAPD structure can achieve an electric field isolation using the unique structure modulation instead of a conventional charge region. The device also had a good behavior of high gain in a wide voltage range, and the dark current in the range remained relatively low. The operating voltage point had a very large range for the novel LAPD, and did not need precise control unlike the classic SACM APDs[20]. Figure 3 shows the E_x and E_y distributions at the Si substrate near the Ge mesa. Gap A in the substrate remained at a high field at -23 V, and the fields in both the mesa region and gap B were relatively low compared with those in the high-field region. The peak point of E_x emerged at $x = -3$ μm, where E_y reached its maximum. The coincident peak of E_x and E_y at $x = -3$ μm showed that the maximum of E_x at the edge of gap A was triggered by the high E_y from the Ge region to the substrate, and the Ge mesa edge and base angle had an enormous influence on the electric field confinement in gap A. Furthermore, the high E_y in the range of gap A drove photo-generated holes in the Ge region to the p^+-doped region. The field in gap A remained higher than 380 kV/cm, and the highest field was 560 kV/cm, which was high enough to trigger the avalanche ionization effect. Moreover, the field in gap B remained lower than 60 kV/cm, indicating that the avalanche gain was triggered in gap A.

We simulated the device without a mesa structure and with a Si mesa taking the place of the Ge mesa to identify the mechanism of the high-field formation in gap A. The peak electric field in the device without mesa emerged at the homo step-junction between the intrinsic substrate and the high-doped region, then linearly decreased toward another side that was highly doped. The high-field location depended on the impurity type of the substrate. In the structure with the Si mesa, the high field was restricted to the gap region with a sharp decrease at the edge of the Si mesa. The location of the high field can be changed from gap A to gap B by altering the type of impurity at Si from n-type to p-type, which was not affected by the impurity type in the intrinsic substrate.

In the comparison of the structure with and without the Si mesa, the mesa region on top of the substrate had an enormous influence on the field distribution in the structure. Meanwhile, the high field in the structure with the Si mesa was formed only on one side of the gap region because of the p-i-n junction formed between the Si mesa and the highly doped region in the substrate. The carriers moving to the other highly doped

region away from the high field drifted into the Si mesa because of the p-i-n junction, which was the reason behind the high-field confinement in the structure with the Si mesa. In the case of the device with the Ge mesa, the high field was limited in gap A, and the location of the high field was not affected by the impurity type in the Si substrate and the top Ge mesa. The result indicated that the mechanism of triggering high field in the structure with Si and Ge mesa was not the same. This eliminated the possibility that the built-in field at the p-i-n junction between the top mesa region and the highly doped Si region triggers the high field in gap A in the device with the Ge mesa.

We simulated the bandgap distribution at the Ge/Si interface to further analyze the mechanism of the high field in gap A. The analysis of the bandgaps in the mesa region showed that a type-II hetero-junction was located at the Ge/Si interface. As shown in Fig. 4a, the hetero-junction structure has two different barriers on electrons and holes, which has a significant influence on the drifted carriers from the Ge mesa to the Si substrate. When the carriers in Ge drifted to the substrate Si, the holes had a larger barrier than the electrons. Figure 4c shows the E_y and current density of the electrons and the holes at $x = 0\,\mu$m. The carrier distribution in the mid region was affected by the build-in field formed by the p-n junction at the Ge/Si interface because of the relatively low field on the vertical direction caused by the bias, which pointed from the n-Si substrate to the p-Ge mesa. Under the effect of the build-in field at the Ge/Si interface, the electrons generated and drifted in mid region were driven to the substrate, and the holes generated in the mid region were driven into the mesa. The hole current density in the Ge mesa was two orders of magnitude higher than the electron current density, which showed a good separation of carriers that drifted by the build-in field in Fig. 4c. As shown in Fig. 3, the E_y in the mesa region along the x direction was relatively uniform, except in the area near gap A. When the holes in the mesa drifted to the mesa edge near gap A by E_x in the Ge mesa, they were blocked by the 0.7 eV barrier on the holes at the Ge/Si hetero junction (Fig. 4b). When the bias was smaller than -22 V, gap A became the main region to bear the bias because of the block effect on the holes at the mesa edge near gap A, forming a steep high-field distribution in gap A. E_y at $x = -3\,\mu$m and E_x in the range of gap A enormously increased, and the electric field distribution exhibited a steep decrease at

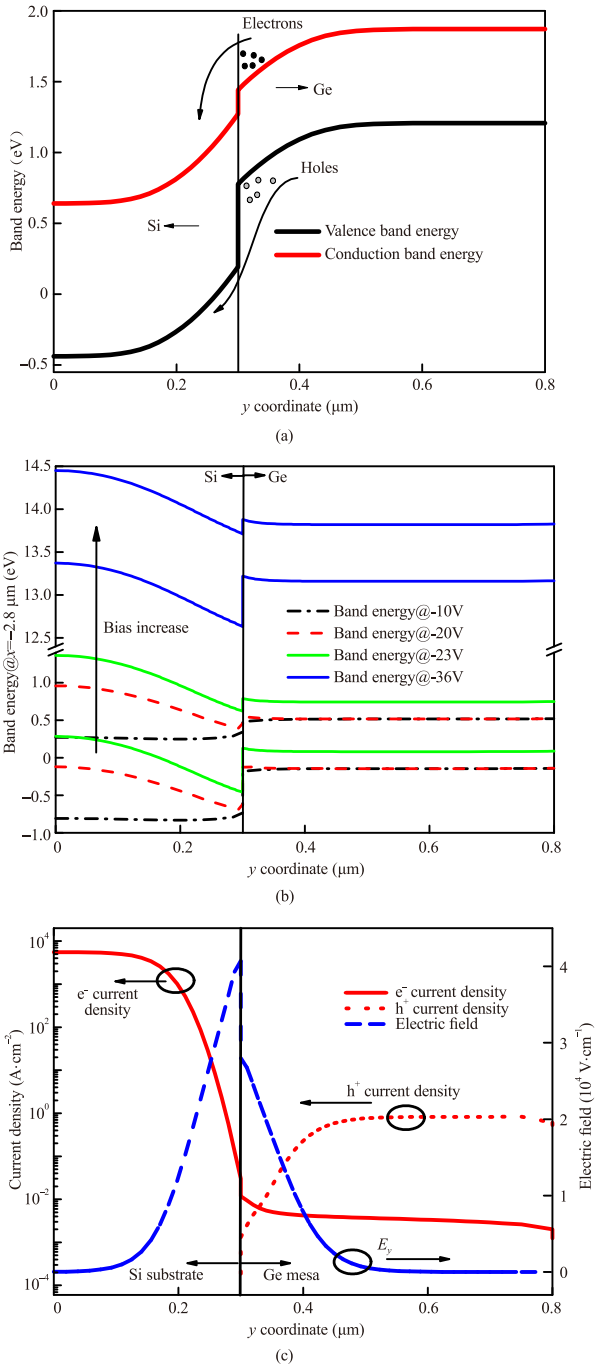

Fig. 4 (a) Bandgap graph at the Si/Ge interface (x = 0 μm) of the device at –23 V. Si substrate concentration $N = 2 \times 10^{16}$ cm^{-3} and Si mesa thickness T = 0 μm. (b) Bandgap energy distribution at the Ge/Si interface near gap A (x = –2.8 μm) under different bias voltages. (c) Electron and hole current density and E_y distribution from the Si substrate to the Ge mesa at x = 0 μm.

$x = +3\,\mu$m. The potential distribution in gap A rose with the increasing bias value, while the other areas in the Si substrate and the Ge mesa retained a low potential distribution, resulting in changing the bandgap bending

in the Si bandgap at the Ge/Si interface and a stable band energy level in the Ge mesa near gap A with the increasing bias (Fig. 4b). Consequently, the photo-generated holes drifting into the high field in gap A triggered the avalanche ionization effect.

After the first electron-hole pairs were generated by the impact of the photo-generated holes from the Ge mesa, the electrons were accelerated in gap A and caused a subsequent impact ionization effect. An enormous gain was generated when the field in gap A was high enough (Fig. 2). The electron flux in Fig. 4c was three orders of magnitude larger than the hole flux because the electron flux was formed by the electrons generated both in the mid region and by the avalanche impact ionization effect in gap A. As shown in Fig. 4b, a barrier in the conduction band in the direction from Si to Ge at the Ge/Si interface near gap A prevented the electrons generated in gap A from drifting into the Ge mesa by reverse bias. The shape of the bandgap at $x = -2.8\,\mu$m kept from changing with the increasing reverse bias when the bias value was larger than –22 V. Moreover, the potential distribution in the other region in the Si substrate started to simultaneously increase, resulting in a stable gain value in the bias range from –23 V to –36 V. The field distribution in gap A decreased when the bias was greater than –36 V because of the space charge effect resulting in the decrease of gain[13]. The value of E_x in the Ge mesa at –23 V remained above 0.5 kV/cm. The relatively low electric field in the x coordinate was caused by the 6 μm-long intrinsic region, which increased the possibility of a recombination of the photo-generated carriers. By shortening the mesa region in the x coordinate to 2 μm and keeping the gap region as 0.5 μm, E_x in the Ge mesa in the bias of the peak increased to 1.1 kV/cm, and the peak gain increased to 305. The electric field in the mid region slowly increased when the bias was above –23 V. In addition, the strength of the electric field in gap A remained steady, which was the reason for the long range of bias of the stable large gain.

Structures with different base angles and thicknesses of the Ge mesa were simulated to further analyze the effect of the Ge mesa shape on the device. The peak gain of the device decreased from 120 to 108 when the base angle of the Ge mesa changed from 26.5° to 90°. Moreover, the electric field in gap A slowly decreased. The base angle shape had a weak influence on the device behavior. E_y in the top Ge mesa region increased with the decrease in the Ge mesa thickness from 1 μm to 0.5 μm. The peak gain simultaneously increased from 63 to 108. The Ge mesa with a larger thickness decreased E_y in the top region of the Ge mesa and reduced the transport of the photo-generated carriers in the mesa region because E_y in the mid region near $x = 0\,\mu$m was formed owing to the hetero junction in the Ge/Si interface. The abovementioned analyses indicated that steep and thin Ge mesa increased the avalanche effect in the device.

The simulation showed that the modulation effect of the Ge/Si interface on the electric field in the device can be enhanced by changing the impurity concentration of the substrate and adding the Si mesa in the structure. We analyzed herein the structure using various substrate impurity concentrations ranging from 4×10^{12} cm^{-3} to 4×10^{16} cm^{-3}. Figure 5a shows the gain change with

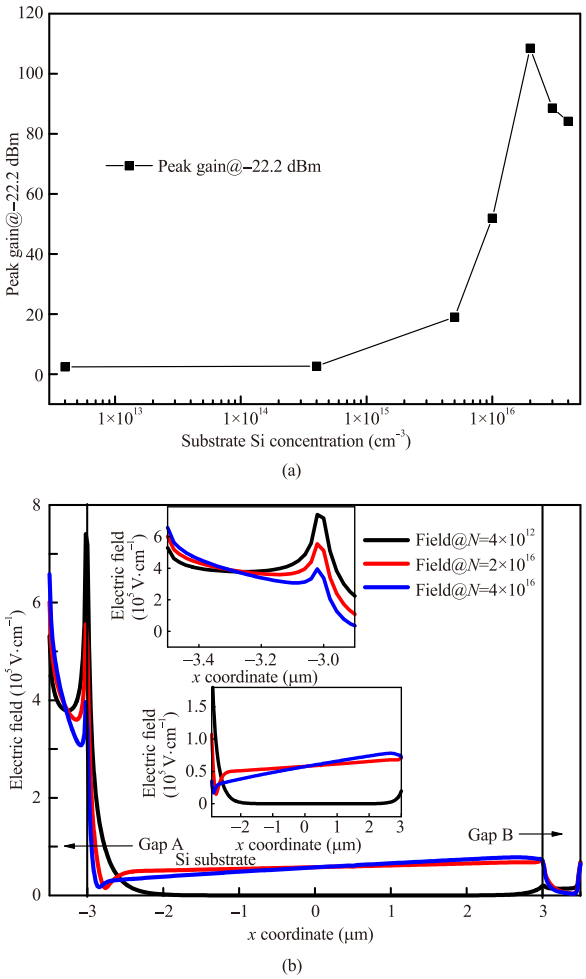

Fig. 5 (a) Peak gain of the device for various substrate concentrations. (b) Electric field distribution in the Si substrate at $y = 0.28\,\mu$m for various substrate concentrations. The upper and lower insets are enlarged figures of the field in gap A and in the center mesa region, respectively, at $y = 0.28\,\mu$m.

respect to the substrate concentration under −22.2 dBm incident light. The gain of the device was below 5 when the impurity concentration N was from $4 \times 10^{12}\,\mathrm{cm}^{-3}$ to $4 \times 10^{14}\,\mathrm{cm}^{-3}$. Although the high field in gap A remained high enough, a relatively low build-in field at the Ge/Si interface weakened the separation between the electrons and the holes in the Ge mesa, resulting in fewer photo-generated holes drifting in the high-field region in gap A (lower inset of Fig. 5b). The gain rapidly increased after N rose above $5 \times 10^{15}\,\mathrm{cm}^{-3}$ and reached a peak value of 108 at $2 \times 10^{16}\,\mathrm{cm}^{-3}$. The built-in field at the Ge/Si interface when the impurity concentration in the substrate was changed was significantly varied and further influenced the whole field distribution in the device. The strengthened build-in field at the Ge/Si interface separated carriers in the Ge mesa, and a larger amount of photo-generated holes remained without recombination and drifted into gap A by E_x in the Ge mesa. As seen in the upper inset of Fig. 5b, the strengthened build-in field at the Ge/Si interface and at the homo step-junction when a higher concentration was applied to the substrate in gap A simultaneously decreased the peak field at $x = -3\,\mu\mathrm{m}$ near the Ge mesa and increased the peak field at $x = -3.5\,\mu\mathrm{m}$ near the p^+-doped region. The lowest field value in gap A was larger than $350\,\mathrm{kV/cm}^{-3}$ when the concentration reached $2 \times 10^{16}\,\mathrm{cm}^{-3}$. This value was big enough to trigger a violent impact ionization in the high-field region of gap A, and the high field at the corner near the mesa region was evidently restrained. The minimum fields in gap A started to decrease and was below 300 when the concentration reached $4 \times 10^{16}\,\mathrm{cm}^{-3}$. The available avalanche length in gap A was less than $0.5\,\mu\mathrm{m}$, leading to a decrease in the avalanche gain of the device (Fig. 5a).

The analysis of the field distribution in the devices showed that the high-average build-in field at the Ge/Si interface influenced the peak gain. The Si mesa between the Ge mesa and the Si substrate was added to achieve a stronger field confinement in the Ge absorption region and push the upper Ge region away from the Si substrate. The changes in the electric field distribution in the Si substrate when the Si mesa was added to the structure were similar to those in the case obtained by varying the substrate impurity concentration (Fig. 6a). The maximum electric field value in gap A increased with the increase in the Si mesa thickness. Moreover, a similar behavior was found compared to the situation shown in Fig. 5b, in which the

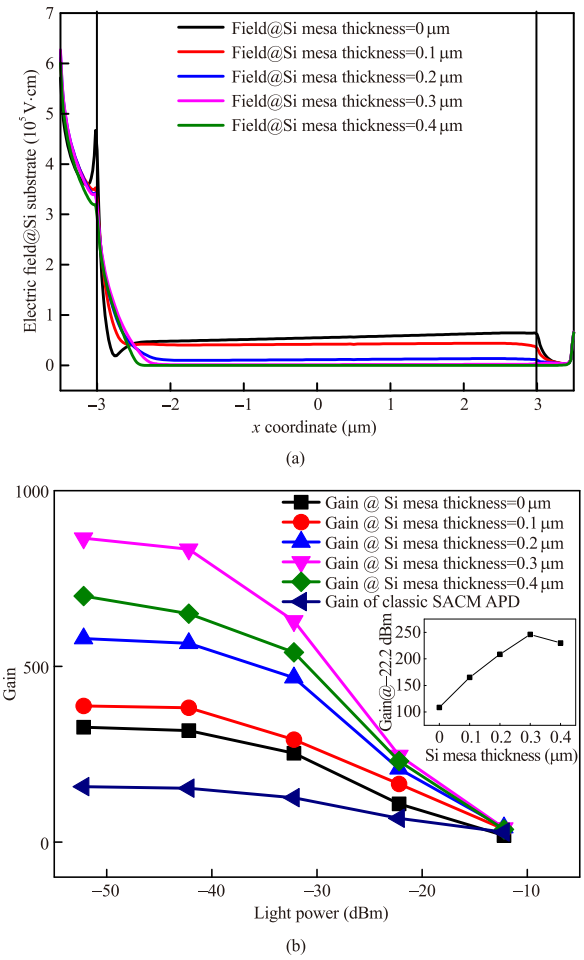

Fig. 6 (a) Electric field distribution in the Si substrate at $y = 0.28\,\mu\mathrm{m}$ for several Si mesa thicknesses. (b) Gain of the device for several Si mesa thicknesses under various incident light powers. A classic vertical SACM APD with the same incident area, absorption, and multiplication length is analyzed for comparison. The inset shows the change in the gain of the device for various Si mesa thicknesses under –22.2 dBm light.

field near the mesa edge evidently decreased. This was caused by the rising distance between the Si substrate and the Ge/Si interface. The high field in the center region was still near the Ge/Si interface and slowly rose with the increasing Si mesa thickness. However, the field in the center region of the substrate decreased because of the larger distance between the substrate and the Ge/Si interface. The rising average field in Ge can impose a more complete separation between the photo-generated electrons and the holes, and drift them toward the two electrodes. The maximum field values in gap A and the Ge region for the Si mesa thickness of $0.3\,\mu\mathrm{m}$ were 627 kV/cm and 56 kV/cm, respectively. The avalanche impact ionization in gap A increased for

the thicker Si mesa, and the avalanche breakdown in Ge was completely limited. The electric confinement was greatly strengthened by adding Si mesa in the structure, surpassing its limit under various substrate concentrations analyzed before. However, the electric confinement was weakened for $T > 0.3\,\mu\text{m}$, because of the decoupled relationship between Ge mesa and gap A. In Fig. 6b, the gain of the device for $T = 0.3\,\mu\text{m}$ shows a large improvement of 2.3 compared with that without Si mesa. The gain sharply increased under a lower light power. For $N = 2 \times 10^{16}\,\text{cm}^{-3}$ and $T = 0.3\,\mu\text{m}$, values of 246 and 865 were reached under incident light powers of –22.2 dBm and –52.2 dBm, respectively. The gain and dark current were satisfied compared with those of a classic vertical SACM APD of the same size in the simulation (Fig. 6b).

4 Conclusion

We studied a new LAPD structure with a novel interface electric confinement mechanism using a simulation. The special bandgap and the build-in electric field characteristics of the Ge/Si interface structure were effective in separating the carriers in the mid region of the device and further induced a high electric field distribution in gap A. The electric field distribution in the structure was well confined using the changed thickness of the Si mesa and the changed impurity concentration in the Si substrate. The whole Ge region was depleted, and the high-field confinement in gap A and the separation of carriers in the Ge mesa were strengthened compared with the structure without modulation. The peak gain of the LAPD reached values of 246 and 865 under incident light powers of –22.2 dBm and –52.2 dBm, respectively, when the Si mesa thickness was $T = 0.3\,\mu\text{m}$ and the impurity concentration in Si was $N = 2 \times 10^{16}\,\text{cm}^{-3}$. The LAPD can be designed to have a large gain and a low dark current through an appropriate modulation of the substrate impurity concentration and the Si mesa thickness. Compared to the SACM APD, the LAPD structure proposed in this study reached a higher gain for the same multiplication length and maintained a high gain at relatively low dark current in a bias range of over –10 V. The large gain value and the wide bias range for multiplication make the proposed LAPD a promising candidate for single photon detection and long-distance photo-communication.

Acknowledgment

This work was supported in part by the National Natural Science Foundation of China (No. 61534005) and Natural Science Foundation of Beijing Municipality (No. 4162063).

References

[1] S. Y. Ke, S. M. Lin, X. Li, J. Li, J. F. Xu, C. Li, and S. Chen, Voltage sharing effect and interface state calculation of a wafer-bonding Ge/Si avalanche photodiode with an interfacial GeO_2 insulator layer, *Opt. Express,* vol. 24, no. 3, pp. 1943–1952, 2016.

[2] Y. Dong, W. Wang, S. Y. Lee, D. Lei, X. Gong, W. K. Loke, S. F. Yoon, G. Liang, and Y. C. Yeo, Avalanche photodiode featuring germanium-tin multiple quantum wells on silicon: Extending photodetction to wavelengths of 2 μm and beyond, in *2015 IEEE International Electron Devices Meeting (IEDM)*, Washington, DC, USA, 2015.

[3] J. Xu, X. S. Chen, W. J. Wang, and W. Lu, Extracting dark current components and characteristics parameters for InGaAs/InP avalanche photodiodes, *Infrared Physics & Technology,* vol. 76, pp. 468–473, 2016.

[4] S. Y. Zhu, K. W. Ang, S. C. Rustagi, J. Wang, Y. Z. Xiong, G. Q. Lo, and D. L. Kwong, Wave-guided Ge/Si avalanche photodiode with separate vertical SEG-Ge absorption, lateral Si charge, and multiplication configuration, *IEEE Electron Device Lett.,* vol. 30, no. 9, pp. 934–936, 2009.

[5] Z. H. Huang, D. Liang, C. Santori, M. Fiorentino, C. Li, and R. G. Beausoleil, Low-voltage Si/Ge avalanche photodiode, in *2015 IEEE 12th International Conference on Group IV Photonics (GFP)*, Vancouver, Canada, 2015.

[6] C. A. Lee, R. A. Logan, R. L. Batdorf, J. J. Kieimack, and W. Wiegmann, Ionization rates of holes and electrons in silicon, *Phys. Rev.,* vol. 134, no. 3A, pp. A761–A773, 1964.

[7] R. J. McIntyre, The distribution of gains in uniformly multiplying avalanche photodiodes: Theory, *IEEE Trans. Electron.,* pp. 703–713, 1972.

[8] Z. H. Huang, C. Li, D. Liang, K. Z. Yu, C. Santori, M. Fiorentino, W. Sorin, S. Palermo, and R. G. Beausoleil, A 25 Gbps low-voltage waveguide Si-Ge avalanche photodiode, in *Conference on Lasers and Electro-Optics, 2016 OSA Technical Digest Series (Optical Society of America, 2016)*, San Jose, CA, USA, 2016.

[9] Y. Kang, H. Liu, M. Morse, M. J. Paniccia, M. Zadka, S. Litski, G. Sarid, A. Pauchard, Y. H. Kuo, and H. W. Chen, et al., Monolithic germanium/silicon avalanche photodiodes with 340 GHz gain-bandwidth product, *Nat. Photon.,* vol. 3, pp. 59–63, 2009.

[10] N. Duan, T. Y. Liow, A. E. Lim, L. Ding, and G. Q. Lo, 310 GHz gain-bandwidth product Ge/Si avalanche photodetector for 1550 nm light detection, *Opt. Express,* vol. 20, no. 10, pp. 11031–11036, 2012.

[11] F. M. Abou El-Ela and I. M. Hamada, Impact ionization coefficients of electron and hole at very high fields in semiconductors, in *Modern Trends in Physics Research, 2005 American Institute of Physics (AIP) Conference Proceedings*, Cairo, Egypt, 2004.

[12] W. Maes, K. D. Meyer, and V. Overstraeten, Impact ionization in silicon: A review and update, *Solid State*

Electron., vol. 33, no. 6, pp. 705–718, 1990.
[13] H. C. Bowers, Space-charge-induced negative resistance in avalanche diodes, *IEEE Trans. Electron. Dev.,* vol. 15, no. 6, pp. 343–350, 1968.
[14] E. Jamil, M. M. Hayat, P. S. Davids, and R. M. Camacho, 3D avalanche multiplication in Si-Ge lateral avalanche photodiodes, in *Advanced Photon Counting Techniques X, 2016 Proceedings of SPIE*, Baltimore, ML, USA, 2016.
[15] J. M. Hartmann, J.M. Fabbri, G. Rolland, A. M. Papon, T. Billon, M. Juhel, and A. Halimaoui, In-situ HCl etching and selective epitaxial growth of Boron-doped Ge for the formation of recessed and raised sources and drains, *Electrochem. Soc. Trans.,* vol. 3, no. 7, pp. 489–500, 2006.
[16] J. C. Irvin, Resistivity of bulk silicon and of diffused layers in silicon, *Bell Labs Tech. J.,* vol. 41, no. 2, pp. 387–410, 1962.
[17] V. A. Shah, A. Dobbie, M. Myronov, and D. R. Leadley, Effect of layer thickness on structural quality of Ge epilayers grown directly on Si (001), *Thin Solid Films,* vol. 519, no. 22, pp. 7911–7917, 2011.
[18] H. U. Kim and S. W. Rhee, Electrical properties of bulk silicon dioxide and SiO_2/Si interface formed by tetraethylorthosilicate-ozone chemical vapor deposition, *J. Electrochem. Soc.,* vol. 147, no. 4, pp. 1473–1476, 1999.
[19] E. Yablonovitch, D. L. Allara, C. C. Chang, T. Gmitter, and T. B. Bright, Unusually low surface-recombination velocity on silicon and germanium surfaces, *Phys. Rev. Lett.,* vol. 57, no. 2, pp. 249–252, 1986.
[20] H. Cong, C. L. Xue, Z. Liu, C. B. Li, B. W. Cheng, and Q. M. Wang, High-speed waveguide-integrated Ge/Si avalanche photodetector, *Chin. Phys. B,* vol. 25, no. 5, p. 052803, 2016.

Wenzhou Wu received the BEng degree from Xidian University, China in 2012. He is currently a PhD student in Institute of Semiconductor, Chinese Academy of Sciences, China. His research interest is silicon photonics, especially silicon based photo-detectors.

Zhi Liu received the BSci degree from Taiyuan University of Technology, China in 2009, and the PhD degree from Institute of Semiconductor, Chinese Academy of Sciences, China in 2014. Since 2014, he has been with Institute of Semiconductor, Chinese Academy of Sciences, China. His research interest is silicon based group IV material growth and silicon photonics. He has authored or co-authored more than 30 journal articles.

Jun Zheng received the BSci degree from Beijing Institue of Technology, China in 2006 and PhD degree in physical electronics from Graduated University of Chinese Academy of Sciences, China in 2011. He is now an associate researcher in Institute of Semiconductor, Chinese Academy of Sciences, China. His research interest is silicon photonics, especially silicon based materials and detectors.

Yuhua Zuo received the BEng and MEng degrees from Tsinghua University, China in 1997 and 2000, respectively, and the PhD degree in microelectronics and optoelectronics from Institute of Semiconductors, Chinese Academy of Sciences, China in 2003. She is a professor in both University of Chinese Academy of Sciences, China and Institute of Semiconductors, Chinese Academy of Sciences. She worked as visiting scholar in Department of Materials, University of California at Los Angeles for 8 months in 2016. She has extensive research expertise and a wide range of research interests in novel Si-based optoelectronics materials and devices, such as PD, APD, and solar cells.

Buwen Cheng received the BS degree and MS degree in condensed physics from Beijing Normal University, China in 1989 and 1992, respectively. In 2006, he received the PhD degree from the Institute of Semiconductors, Chinese Academy of Sciences (ISCAS), China. He joined the ISCAS in 1992. Since 2007, he has been a professor. His current research interests include growth of Si-based materials (such as SiGe, Ge, and GeSn) and device applications. He has authored or co-authored more than 150 journal articles and holds 15 patents.